Available online at www.sciencedirect.com
ScienceDirect
Journal of Power Sources 179 (2008) 770–779
JOURNAL OF POWER SOURCES
www.elsevier.com/locate/jpowsour

Electrochemical properties and lithium ion solvation behavior of sulfone–ester mixed electrolytes for high-voltage rechargeable lithium cells

Yuu Watanabe, Shin-ichi Kinoshita, Satoshi Wada, Keiji Hoshino, Hideyuki Morimoto, Shin-ichi Tobishima *

Department of Chemistry, Faculty of Engineering, Gunma University, 1-5-1 Tenjincho, Kiryu, Gunma 376-8515, Japan

Received 12 October 2007; received in revised form 25 December 2007; accepted 4 January 2008
Available online 11 January 2008

Abstract

Sulfone–ester mixed solvent electrolytes were examined for 5 V-class high-voltage rechargeable lithium cells. As the base-electrolyte, sulfolane (SL)–ethyl acetate (EA) (1:1 mixing volume ratio) containing 1 M $LiBF_4$ solute was investigated. Electrolyte conductivity, electrochemical stability, Li^+ ion solvation behavior and cycleability of lithium electrode were evaluated. ^{13}C NMR measurement results suggest that Li^+ ions are solvated with both SL and EA. Charge–discharge cycling efficiency of lithium anode in SL–EA electrolytes was poor, being due to its poor tolerance for reduction. To improve lithium charge–discharge cycling efficiency in SL–EA electrolytes, following three trials were carried out: (i) improvement of the cathodic stability of electrolyte solutions by change in polarization through modification of solvent structure; isopropyl methyl sulfone and methyl isobutyrate were investigated as alternative SL and EA, respectively, (ii) suppression of the reaction between lithium and electrolyte solutions by addition of low reactivity surfactants of cycloalkanes (decalin and adamantane) or triethylene glycol derivatives (triglyme, 1,8-bis(*tert*-butyldimethylsilyloxy)-3,6-dioxaoctane and triethylene glycol di(methanesulfonate)) into SL–EA electrolytes, and (iii) change in surface film by addition of surface film formation agent of vinylene carbonate (VC) into SL–EA electrolytes. These trials made lithium cycling behavior better. Lithium cycling efficiency tended to increase with a decrease in overpotential. VC addition was most effective for improvement of lithium cycling efficiency among these additives. Stable surface film is formed on lithium anode by adding VC and the resistance between anode/electrolyte interfaces showed a constant value with an increase in cycle number. When the electrolyte solutions without VC, the interfacial resistance increased with an increase in cycle number. VC addition to SL–EA was effective not only for $Li/LiCoO_2$ cell with charge cut-off voltage of 4.5 V but also for $Li/LiNi_{0.5}Mn_{1.5}O_4$ cells even with high charge cut-off voltage of 5 V in $Li/LiNi_{0.5}Mn_{1.5}O_4$ cells.

Keywords: Lithium cell; Electrolyte; Sulfone; Ester; Solvation

1. Introduction

4 V-class lithium-ion cells have been commercially applied for electronic portable equipments such as cellular phones and note-type personal computers. However, lithium-ion cells are extending their new uses such for electric vehicles and power storage batteries. These equipments need higher voltage cells such as 5–6 V discharge as well as more larger charge–discharge capacity and higher energy density. To increase the cell voltage, it is important not only development of new electrode materials but also improvement of new electrolytes having higher anodic stability than conventional electrolytes using solvents such as ethylene carbonate (EC), propylene carbonate (PC), diethyl carbonate (DEC), dimethyl carbonate (DMC) and ethyl methyl carbonate (EMC). There have been many studies to develop new electrolytes for high-voltage lithium cells [1–5]. For example, fluorinated carbonate solvents exhibit higher anodic stability, relative permittivity and viscosity [1,2]. Nitrile solvents show high anodic stability and low viscosity [3,4]. Ionic liquids are also known to show higher anodic stability, noncombustible and high ionic conductivity. Especially, aliphatic ammonium bis(trifluoromethanesulfone)imide show superior anodic stability [5]. However, charge–discharge properties, cathodic stability and compatibility for lithium anode of there solvents have not been investigated clearly.

Sulfones are investigated for high-voltage cells due to their anodic stability [6–8]. SL is a common solvent known to show high anodic stability, high relative permittivity. However, SL is

* Corresponding author. Tel.: +81 277 30 1382; fax: +81 277 30 1380.
E-mail address: tobi@chem-bio.gunma-u.ac.jp (S.-i. Tobishima).

0378-7753/$ – see front matter © 2008 Elsevier B.V. All rights reserved.
doi:10.1016/j.jpowsour.2008.01.006

Fig. 1. Chemical structure of sulfolane and ethyl acetate.

solid at room temperature, and its viscosity is too high at liquid phase. EA is also very common as an organic solvent. It has good anodic stability and low viscosity, but its relative permittivity is only 6.02 at 25 °C [9]. It is too low to dissociate supporting salts enough. In addition, generally, a solvent shows high relative permittivity and high viscosity is mixed with other solvent shows low relative permittivity and low viscosity to obtain preferable properties.

In this work, sulfone–ester mixed solvent electrolytes were examined for 5 V-class high-voltage rechargeable lithium cells. As the base-electrolyte, SL–EA mixed solvent containing $LiBF_4$ solute was investigated. $LiBF_4$ is used here because tolerance of $LiBF_4$ toward oxidation is reported to be higher than that of $LiPF_6$ [10]. Fig. 1 shows chemical structure of two solvents, SL as cyclic sulfone, and EA as ester. Table 1 shows physical properties of these solvents.

In this study, oxidation potential (E_{ox}), reduction potential (E_{red}), and charge–discharge cycling performance of lithium using Li/Pt and Li/$LiCoO_2$ cells were evaluated. Li^+ solvation behavior was investigated by estimation of Stokes' radius (r_s) and ^{13}C NMR measurements. To improve lithium charge–discharge cycling efficiency with SL–EA electrolytes, we carried out following three trials: (i) improvement of the cathodic stability of electrolyte solutions by change in polarization through modification of solvent structure; isopropyl methyl sulfone and methyl isobutyrate were investigated as alternative SL and EA, respectively, (ii) suppression of the reaction between lithium and electrolyte solutions by addition of low reactivity surfactants of cycloalkanes (decalin and adamantane) or triethylene glycol derivatives (triglyme, 1,8-bis(*tert*-butyldimethylsilyloxy)-3,6-dioxaoctane and triethylene glycol di(methanesulfonate)) into SL–EA electrolytes, and (iii) change in surface film by addition of surface film formation agent of vinylene carbonate into SL–EA electrolytes.

2. Experimental

2.1. Preparation of electrolyte solutions

Battery grade of $LiBF_4$ and SL, EA, PC, EC, EMC, triethylene glycol dimethyl ether (triglyme) and vinylene carbonate (VC) were obtained from Tomiyama Pure Chemicals. Adamantane (Aldrich Chemical Company) which is dissolved in test electrolyte and neat decalin (Wako Pure Chemical Industry) were dried over molecular sieves 3A for 3 days. 1,8-Bis(*tert*-butyldimethylsilyloxy)-3,6-dioxaoctane (TBDMSO) and triethylene glycol di(methanesulfonate) (TriglyMs) were prepared by the following method and identified as literatures [14,15].

Our electrolyte solutions were prepared as described in a previous paper [16,17]. The water content of the test solutions was less than 20 ppm as determined by the Karl–Fisher titration method. Hereafter, "1 M $LiBF_4$/SL–EA (1:1)" represents the mixed SL and EA solvents (mixing volume ratio = 1:1) dissolved in 1 M (M: mol L^{-1}) $LiBF_4$.

2.1.1. Preparation of TBDMSO

1.50 g (10.0 mmol) of triethylene glycol, 1.83 g (15.0 mmol) of dimethylaminopyridine are mixed with 10 mL of DMF in argon-filled three-necked flask with condenser. 3.02 g (20.0 mmol) of *tert*-butyldimethylsilyl chloride dissolved with 5 mL of DMF was dropped into the flask for 10 min under cooling with ice-water. The mixture was stirred for 7 h at room temperature, poured into ice-water, extracted with 20 mL of diethyl ether for three times. The crude product was chromatographed with hexane–ethyl acetate (volume ratio 5:1) mixed eluent, then 2.29 g of light yellow liquid product was obtained (yield 61%).

^1H NMR: 0.06 (s, 12H), 0.89 (s, 18H), 3.56 (t, 4H, J = 5.4 Hz), 3.64 (s, 4H), 3.77 (t, 4H, J = 5.4 Hz).

2.1.2. Preparation of TriglyMs

1.65 g (11.0 mmol) of triethylene glycol, 2.52 g (24.9 mmol) of triethylamine and 10 mL of benzene are put in argon-filled three-necked flask with condenser. 2.85 g (24.9 mmol) of methanesulfonyl chloride diluted with 5 mL of benzene was added drop by drop for 30 min with stirring. The mixture was stirred for 6 h at room temperature. The mixture was filtered, washed with 30 mL of mixed solvent of dichloromethane and benzene (volume ratio 1:1), ice-water for two times, saturated NaCl water for two times, dried over dehydrated $MgSO_4$. After removal of solvent, the crude product was stirred with 2 mL of diethyl ether vigorously. 2.94 g of yellow oil product was obtained by decantation of diethyl ether (yield 87%).

^1H NMR: 3.07 (s, 6H), 3.68 (s, 4H), 3.77 (m, 4H), 4.37 (m, 4H).

Table 1
Relative permittivity (ε), viscosity (η), donor number (DN), acceptor number (AN), melting point (mp) and boiling point (bp) of SL and EA

Solvent	ε	η (cP)	DN	AN	mp (°C)	bp (°C)
SL	60 (20 °C) [6], 43.3(30 °C) [9]	10.29 (30 °C) [9]	14.8 [11]	19.0 [12]	27 [6]	285 [6]
EA	6.02 (20 °C) [9]	0.449 (20 °C) [9]	17.1 [12]	–	−84 [9]	77 [9]
PC	69 (23 °C) [9]	2.5 [13]	15.1 [13]	–	−49 [9]	242 [9]
EC	90 (40 °C) [13]	1.92 (40 °C) [9]	16.4 [13]	–	36 [9]	238 [9]
EMC	2.9 (25 °C) [13]	0.65 [13]	–	–	−55 [13]	108 [13]

2.2. Measurement of electrochemical and physical properties

All the test cells were prepared in argon gas-filled glove box. Measurements of E_{ox} and E_{red} were carried out at 25 °C with cylindrical glass cells with working electrode (Pt sheet, 0.15 cm^2 in area, 0.1-mm thick) and Li metal sheet (0.04 cm^2 in area, 0.1-mm thick) pressed on Ni mesh (200 mesh, 0.15 cm^2 in area, 0.1-mm thick) as reference and counter electrode [16]. E_{ox} and E_{red} values were evaluated as the voltage at the intersection of the *x*-axis baseline (voltage) and the tangent of the rapid increase in the current curve by liner sweep voltammetry.

Charge–discharge cycling test was performed galvanostatically with glass cells or coin cells. Glass cells were assembled with a Pt electrode (0.1-mm thick, 0.15 cm^2 in area) as a working electrode, a Li metal sheet (0.04 cm^2, 0.1-mm thick) pressed on Ni mesh (200 mesh, 0.15 cm^2 in area, 0.1-mm thick) as a counter. Although Pt electrode is able to form alloy with lithium metal, the values of Li charge–discharge cycling efficiency were discussed from relative values among electrolytes in this study. Coin cells (2032 type, 20 mm in diameter, 3.2 mm in thickness) are composed of the printed $LiCoO_2$ or $LiNi_{0.5}Mn_{1.5}O_4$ electrode prepared by coating an Al sheet with a mixture of carbon powder and poly(vinylidene fluoride) (PVdF).

^{13}C NMR spectra were obtained by JEOL α-300 (^1H at 300 MHz). Viscosity was measured with Ostwald viscometer. Molar conductivity of electrolyte solutions was measured with symmetry cell with platinum black electrodes by ac impedance method. Cation transference number was evaluated by measurement of electromotive force (*E*) with concentration cells (Eq. (1)) [18], where Eq. (2), *R*: gas constant, *T*: temperature, *F*: Faraday constant, t_-: transference number of anion ($t_+ + t_- = 1$), *f*: activity coefficient (assumed to 1).

$$\mathrm{Li}|C_1\ \mathrm{mol\,L^{-1}}||C_2\ \mathrm{mol\,L^{-1}}|\mathrm{Li} \quad (1)$$

$$E = \frac{2RT}{F} t_- \ln \frac{C_1 f_1}{C_2 f_2} \quad (2)$$

3. Results and discussion

3.1. Fundamental properties of SL–EA electrolytes

3.1.1. Conductivity of SL–EA electrolytes

Fig. 2 shows relationships among the mixing ratio of SL, conductivity (κ) and viscosity of 1 M $LiBF_4$/SL–EA electrolytes. The maximum value of conductivity (κ_{max}), 2.2 mS cm^{-1} appeared at the SL:EA = 50:50 (vol.%). The reason why κ_{max} is obtained is explained as follows. Conductivity is proportional to the product of number of free ions (i.e., ionic dissociation degree of solute) and migration speed of ions. When the kind of solute and its concentration is fixed, ionic dissociation degree of solute and migration speed of ions is affected mainly by dielectric constant of solvent and viscosity of solution, respectively. As mentioned before, SL has high dielectric constant and viscosity and EA has low dielectric constant and viscosity. In 1 M $LiBF_4$/SL–EA mixed solvent electrolytes, the dielectric constant linearly increases with an increase in a mixing volume ratio of SL. Due to the high viscosity of SL, the viscosity of the mixed solvent electrolytes increased with an increase in the mixing ratio of SL as shown in Fig. 2. Then, the κ_{max} is resulted from the total effects of change in dielectric constant and viscosity. The highest conductive composition, 1 M $LiBF_4$/SL–EA (50:50) was used for the following experiments.

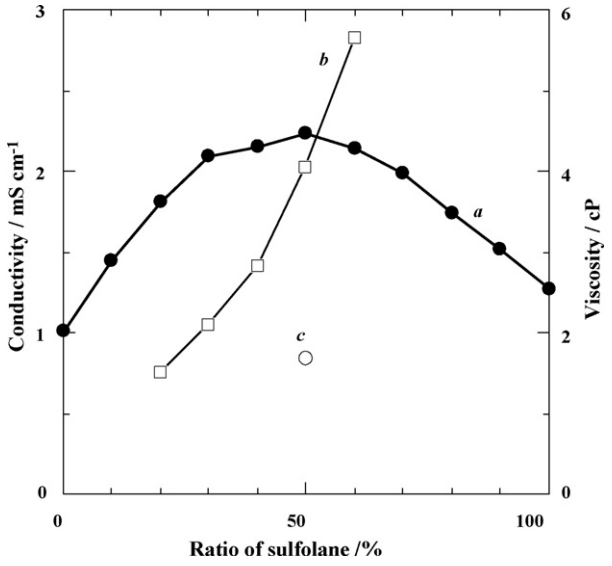

Fig. 2. Relationships among the ratio of sulfolane in 1 M $LiBF_4$/SL–EA electrolyte and conductivity and viscosity (25 °C), a(●): conductivity of 1 M $LiBF_4$/SL–EA, b(□): viscosity of 1 M $LiBF_4$/SL–EA and c(○): viscosity of SL–EA (50:50) solvent.

3.1.2. Electrochemical stability of SL–EA electrolytes

Oxidation and reduction behavior of SL, EA and SL–EA electrolytes are shown in Fig. 3 with EC–EMC electrolytes. EC–EMC electrolytes is a typical electrolyte for 4.2 V charging lithium ion cells and is used here as reference electrolyte.

Anodic current of SL is very small until 6 V *vs.* Li/Li^+. Oxidation starts at 4.9 V *vs.* Li/Li^+ for EA. Distinct anodic current flows at 5.9 V *vs.* Li/Li^+ for SL–EA. SL–EA mixed solvent electrolyte shows intermediate oxidation behavior between SL and EA single solvent electrolytes. EC–EMC starts to be oxidized at 4.1 V *vs.* Li/Li^+ and current gradually increases with an increase in voltage. The oxidation tolerance is ordered in SL > SL–EA > EA > EC–EMC. Table 2 shows the relation between oxidation potential (E_{ox}) of SL and EA. Although aliphatic esters are not very stable on electrochemical window, in our study, SL–EA electrolytes shows higher anodic stability than EA electrolyte. Tolerance of reduction is ordered in SL > EC–EMC > EA > SL–EA (Fig. 3(A)) (reduction potential (E_{red}) is ordered in SL–EA > EA > EC–EMC > SL as shown in

Table 2
Redox properties of electrolytes

Solvent	E_{red}/V *vs.*	E_{ox}/V *vs.* Li/Li^+
SL	0.35	5.97
EA	0.90	4.98
SL–EA (1:1)	0.94	5.99
EC–EMC (3:7)	0.69	4.08

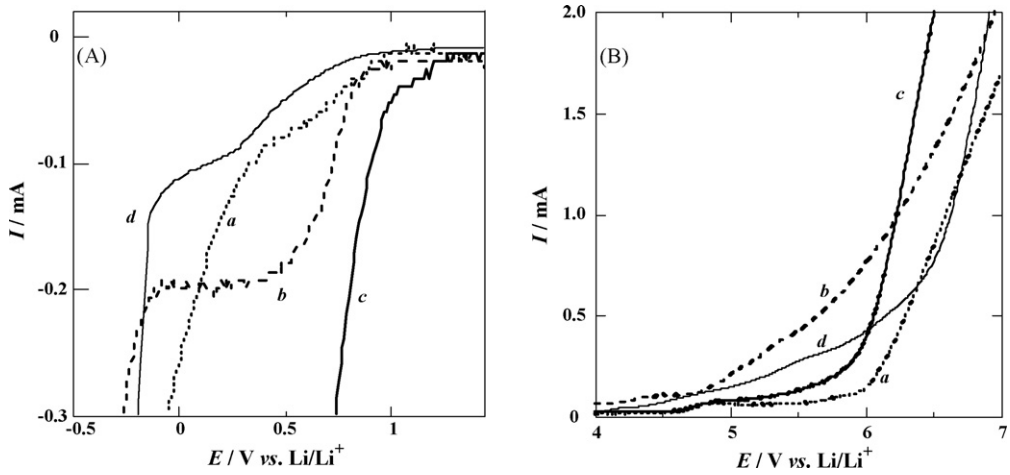

Fig. 3. (A) Reduction and (B) oxidation behavior of electrolytes, supporting electrolyte: 1 M Bu_4NBF_4, a(—): SL, b(– – –): EA, c(—): SL–EA(1:1), d(—): EC–EMC (3:7), (A) scan rate: 10 mV s^{-1}, (B) scan rate: 50 mV s^{-1}.

Table 2). The electrochemical window of SL–EA is *ca.* 1–6 V *vs.* Li/Li^+.

Among electrolytes of SL, EA and SL–EA with 1 M $LiBF_4$, SL–EA system shows highest conductivity and relatively higher E_{ox}.

3.1.3. Solvation behavior of Li^+ ions in SL–EA electrolytes

Lithium cations (Li^+ ions) are solvated with organic solvents in nonaqueous electrolyte solutions. Because positive charge is localized on small Li^+ ions. Solvation means the formation of coordination bond between positive charge of Li^+ ions and relatively high electron charge density part, such as C=O or C–O, of polar solvents. In this work, ^{13}C NMR measurements were carried out to investigate the solvation behavior of Li^+ ions (interactions between solvents and Li^+ ions) in SL–EA solvents. Solvation of cations causes deshielding ^{13}C NMR signals of carbon atoms next to oxygen atoms of solvents [19,20]. This phenomenon is detected by the change in chemical shift values of carbon atoms next to oxygen atoms.

Fig. 4 indicates the influence of concentration of $LiBF_4$ on chemical shift (δ) values of carbon atoms in EA, SL and SL–EA (1:1) electrolytes.

First, the results of $LiBF_4$–EA single solvent electrolytes are discussed. Solvation power of EA towards Li^+ ions may be a little bit stronger than those of EC and PC, very common solvents for lithium cells. Because donor number (DN) of EA, EC and PC is 17.1, 16.4 and 15.1, respectively (Table 1). According to Fig. 4(A), δ values of carbon atoms of C2 and C3 of EA show deshielding. Especially δ change of C2 shows a large value of +1.6 ppm at 1 M Li^+ concentration. This result suggests that most Li^+ ion is solvated by oxygen atom of polar carbonyl group of EA.

Second, the results of $LiBF_4$–SL single solvent electrolytes are discussed. Solvation power of SL towards lithium ions may be a little bit weaker than those of EC and PC. Li^+ ions are solvated with SL through its polar sulfonyl group (–SO_2–). Change in polarization between S and O atoms is dominant for the change in interactions between Li^+ ions and SL when the solute concentration changes. However, chemical shift values of carbon atoms of SL do not change notably with a change in $LiBF_4$ concentration (Fig. 4 (B)). Then, it is difficult to detect a change in interactions between Li^+ ions and SL by change in ^{13}C NMR chemical shifts.

Third, the results of $LiBF_4$/SL–EA mixed solvent electrolytes are discussed. The change of chemical shift of SL–EA mixed

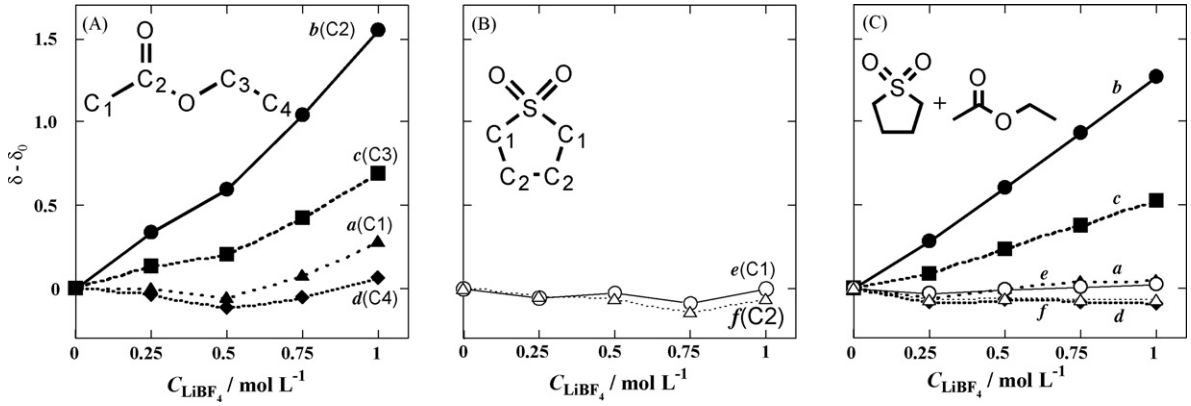

Fig. 4. Influence of Li^+ solvation on ^{13}C NMR chemical shift of solvent, (A) EA, (B) SL, (C) SL–EA (1:1), a(▲): C1 of EA, b(●): C2 of EA, c(■): C3 of EA, d(♦): C4 of EA, e(◯): C1 of SL, f(□): C2 of SL.

solvent is shown in Fig. 4(C). The chemical shift of C2 of EA is deshielding. However, chemical shift change of C2 of EA was +1.3 ppm in SL–EA (1:1) solvent at Li^+ = 1.0 M. This value corresponds to the case of 0.8 M Li^+ in $LiBF_4$–EA single solvent electrolyte solution (Fig. 4(A)). Therefore, Li^+ ions exist in mixed solvation state in SL–EA mixed solvents. 0.8 M of Li^+ may be solvated by EA and the residue 0.2 M Li^+ may be solvated by SL in 1 M $LiBF_4$/SL–EA mixed solvent electrolytes. This assumption is supported by a fact that the donor number (DN) of EA (17.1) is higher than DN of SL (14.8).

3.1.4. Stokes' radius of Li^+ ions in SL–EA electrolytes

Next, the Stokes' radius (r_s) which reflects the size of solvated cation and number of solvating molecules for Li^+ ions in SL–EA electrolytes were estimated. Stokes' radius of Li^+ ions in infinitely diluted condition was calculated by measurements of cation transference number, molar conductivity and viscosity (Eq. (3)). In Eq. (3), z is the valence of cation, q is elementary electric charge and u_+^∞ is the mobility of cation at infinitely dilution condition. When resulting r_s values are relatively small, they were corrected by coefficient (C) described in literature [21].

$$r_s = \frac{zq}{6\pi u_+^\infty \eta} C \tag{3}$$

Fig. 5 shows the electromotive force of concentration cell with SL–EA or EC–EMC electrolyte. Transference number values of Li^+ ions at infinitely dilution condition (t_+^∞) of SL–EA and EC–EMC are 0.63 and 0.58, respectively. t_+^∞ value of EC–EMC is near to the reported value of EC–DEC, 0.5 [22]. Viscosity (η) of SL–EA (1:1) and EC–EMC (3:7) solvent were 1.68 cP and 1.07 cP, respectively. Fig. 6 is the plot of molar conductivity (Λ) against of square root the Li^+ concentration to obtain $u_+{}^\infty$. Λ^∞ of SL–EA is 19.4 mS cm^2 mol^{-1}; EC–EMC is 40.5 mS cm^2 mol^{-1}. Lower conductivity of SL–EA electrolytes is due to the higher viscosity of SL–EA solvent

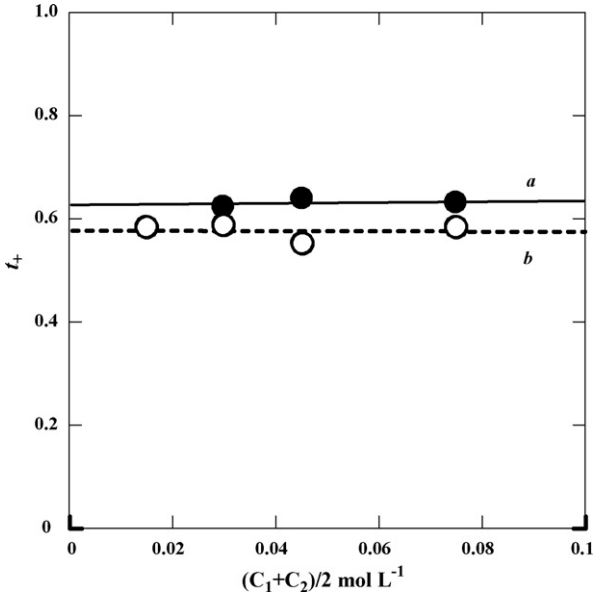

Fig. 5. Measurement of transference number (t_+), supporting electrolyte: $LiBF_4$, a(●): SL–EA (1:1), b(◯): EC–EMC(3:7), 30 °C.

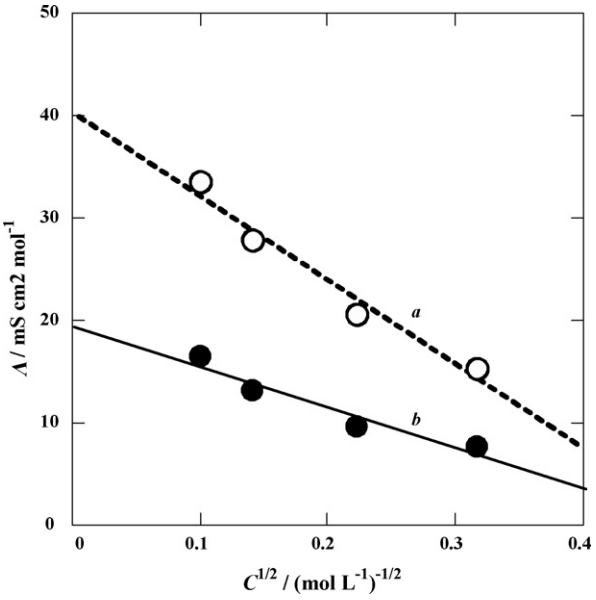

Fig. 6. Measurement of molar conductivity (Λ), supporting electrolyte: $LiBF_4$, a(●): SL–EA (1:1), b(◯): EC–EMC (3:7), 30 °C.

than that of EC–EMC. From these values, r_s of SL–EA is estimated as 0.404 nm and r_s of EC–EMC is 0.327 nm. r_s values applied correction coefficients [21] and molecular volumes are 0.444 nm, 0.367 nm^3 (SL–EA) and 0.420 nm, 0.310 nm^3 (EC–EMC). Then, numbers of solvent molecules solvating to Li^+ ion are estimated. Molecular volume values of SL and EA calculated from their density and molecular weight are 0.158 nm^3 and 0.162 nm^3, respectively. According to the above results of ^{13}C NMR measurement and, 0.8 M Li^+ ions are solvated with EA and 0.2 M Li^+ ions are solvated with SL in 1 M $LiBF_4$/SL–EA electrolytes. Average volume of Li^+ ion with n molecules of solvates in SL–EA (0.367 nm^3) is described as Eq. (4).

$$(0.2 \times 0.158 + 0.8 \times 0.162)n = 0.367 \tag{4}$$

In Eq. (4), $n = ca.$ 2.3. Then, one Li^+ ion is solvated by two or three solvate molecules. The Li^+ ion in mixed solvation state can be described as, i.e. $[Li(SL)_2]^+$, $[Li(SL)(EA)]^+$, and $[Li(EA)_2]^+$. The average value of n, m for $[Li(SL)_n(EA)_m]^+$ are 0.5 and 1.8, respectively. According to ESI-MS studies of solvation behavior of Li^+ with PC and γ-butyrolactone (GBL) solutions, for instance, $[Li(GBL)_2]^+$ and $[Li(GBL)_3]^+$ peaks were observed in 1 mM $LiBF_4$/GBL–MeOH (1:9 (v/v)), and $[Li(EC)_2]^+$ and $[Li(EC)_3]^+$ peaks appeared [23,24]. The number of solvate estimation in SL–EA electrolytes resulted in our study is near to the case of GB and EC–EMC systems in these reports.

3.2. Charge–discharge cycling properties of Li/Pt and Li/$LiCoO_2$ cells with various SL–EA-based electrolytes

3.2.1. Charge–discharge cycling efficiency of Li/Pt and Li/$LiCoO_2$ cells with SL–EA electrolytes

Charge–discharge cycling tests were carried out for Li/Pt and Li/$LiCoO_2$ cells with 1 M $LiBF_4$/SL–EA (1:1) electrolytes

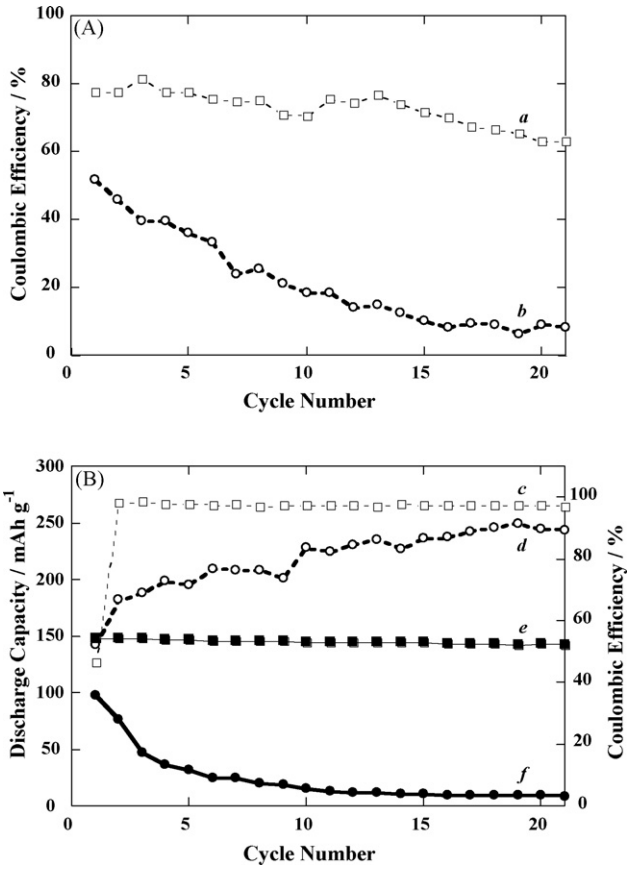

Fig. 7. (A) Coulombic efficiency of Li/Pt cell (supporting electrolyte: 1 M $LiBF_4$, current density: 11 mA cm^{-2}), a(□): EC–EMC (3:7), b(◯): (B) Coulombic efficiency and discharge capacity of Li/$LiCoO_2$ cell (supporting electrolyte: $LiBF_4$, current density: 0.5 mA cm^{-2}, cut-off potential: 3–4.3 V), c(□): EC–EMC (3:7) (Coulombic efficiency), d(◯): SL–EA (1:1) (Coulombic efficiency), e(■): EC–EMC (3:7) (discharge capacity), f(●): SL–EA (1:1) (discharge capacity).

(Fig. 7). Li/Pt cells were used to investigate charge–discharge cycling efficiency of lithium anodes. Li/$LiCoO_2$ cell with SL–EA electrolytes shows a rapid decrease of discharge capacity compared with the cell with EC–EMC electrolytes. Also, Li/Pt cells using SL–EA electrolytes causes a drastic decrease of Coulombic efficiency (charge–discharge cycling efficiency) compared to EC–EMC electrolytes. This result tends to be similar to that obtained in Li/$LiCoO_2$ cells. Then, the cause of a poor cycleability of Li/$LiCoO_2$ cell with SL–EA electrolytes is due to poor cycling efficiency of lithium anode. As mentioned before, the high reduction reactivity of SL–EA toward lithium is most possible reason for poor lithium cycleability. High reduction reactivity of electrolytes makes various factors change which considerably affect lithium cycling efficiency. First example of these factors is lowering lithium cycling efficiency by large consumption of lithium (formation of large amounts of electrochemically inert lithium) based on high reaction rate and high reduction potential. Second example is a drastic change in physical properties of the surface film on lithium anode formed by the reaction between lithium and different electrolyte solutions. In the latter case, the reaction amounts of lithium do not always affect lithium cycling efficiency. In case of SL–EA electrolytes, SL–EA is reduced on lithium anode and then high resistance film may generate.

Isopropyl Methyl Sulfone (IPMS) Methyl Isobutyrate (MIB)

Fig. 8. Chemical structure of isopropyl methyl sulfone and methyl isobutyrate.

3.2.2. Attempt of improvement of charge–discharge cycling properties of SL–EA electrolytes

To improve the charge–discharge cycling efficiency of Li/Pt cell with SL–EA electrolytes by change in cathodic behavior of electrolyte solutions, we made following three trials: (i) improvement of the cathodic stability of electrolyte solutions by change in polarization through modification of solvent structure: isopropyl methyl sulfone (IPMS) and methyl isobutyrate (MIB) were investigated as alternative SL and EA, respectively, (ii) suppression of the reaction between lithium and electrolyte solutions by addition of low reactivity surfactants of cycloalkanes (decalin and adamantane) or triethylene glycol derivatives (triglyme, 1,8-bis(*tert*-butyldimethylsilyloxy)-3,6-dioxaoctane (TBDMSO) and triethylene glycol di(methanesulfonate) (TriglyMs)) into SL–EA electrolytes, and (iii) change in surface film by addition of surface film formation agent of vinylene carbonate (VC) into SL–EA electrolytes.

3.2.2.1. Improvement of cathodic stability of solvents. When the electrolyte solution is reduced at the surface of lithium anode, electrochemically deposited fresh lithium is consumed by chemical reduction. It causes decreasing Coulombic efficiency of lithium anode. Then, chemical structure of solvent was reconsidered from a cathodic stability point of view. Fig. 8 shows the chemical structure of two alternative solvents of SL or EA, isopropyl methyl sulfone (IPMS) and methyl isobutyrate (MIB). In both solvents, isopropyl group having more effective electron-donating property than SL and EA is connected to sulfonyl or carbonyl group. When IPMS or MIB is used as replacement of SL or EA, they are expected to show superior cathodic stability than SL–EA electrolytes.

Oxidation and reduction behavior of 1 M $LiBF_4$/SL–MIB (1:1) and 1 M $LiBF_4$/IPMS–EA (1:1) electrolytes are shown in Fig. 9. SL–MIB is more stable solvent on reduction than SL–EA. Cathodic stability of IMPS–EA does not so differ to SL–EA. SL–MIB, IPMS–EA and SL–EA showed similar oxidation behavior.

Fig. 10 shows Coulombic efficiency of Li/Pt cells with SL–MIB, IPMS–EA and SL–EA electrolytes. IPMS–EA electrolytes exhibited higher Coulombic efficiency than the other two electrolytes. SL–MIB electrolytes showed lower Coulombic efficiency than SL–EA in spite of higher cathodic stability of SL–MIB than SL–EA. Then, properties of reduction products are considered to affect lithium cycling efficiency more strongly than the reduction potential. One of these properties of reduction products is detected to be as overpotential. Table 3 indicates overpotential values at the end of charge and at the

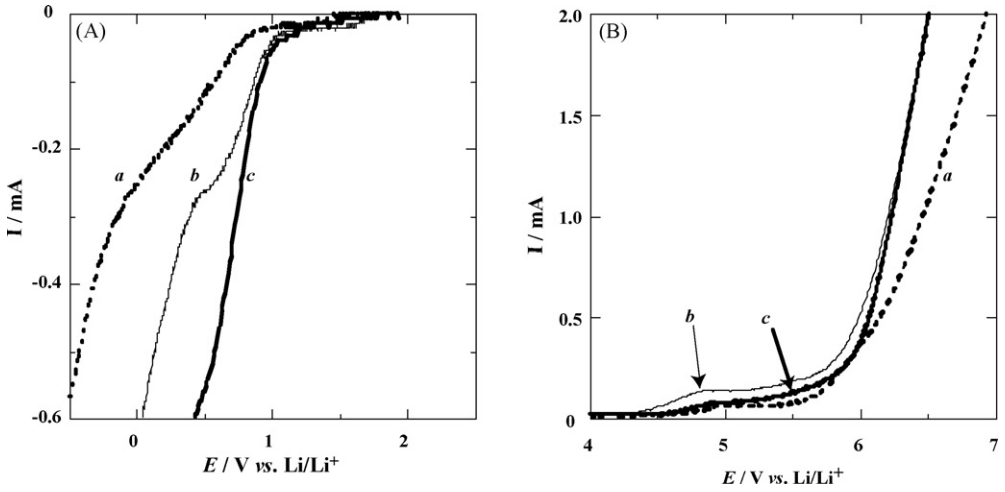

Fig. 9. (A) Reduction and (B) oxidation behavior of electrolytes, a(—): SL–MIB (1:1), b(—): IPMS–EA (1:1), c(—): SL–EA (1:1), (A) scan rate: 10 mV s^{-1}, supporting electrolyte: 1 M Bu_4NBF_4, (B) scan rate: 50 mV s^{-1}, supporting electrolyte: 1 M $LiBF_4$ (a and b) and 1 M Bu_4NBF_4 (c).

start of discharge of Li/Pt cells. Overpotential at both charge and discharge of Li/Pt cell with IPMS–EA electrolytes is lower than SL–EA cell. Overpotential of both charge and discharge of Li/Pt cell with SL–MIB cell is higher than SL–EA cell. Coulombic efficiency of lithium tends to increase with a decrease in an overpotential

Mechanism of decrease in Coulombic efficiency of lithium with sulfone–ester may be explained as follows. Overpotential reflects the resistance of Li electrode surface film generated by the reduction of electrolyte. Higher overpotential of charge causes the dendrite form morphology of electrodeposited Li. Coulombic efficiency should be lowered by suppression of dendrite. Therefore, next, we try to lower the resistance of Li surface film by addition of low reactivity surfactants into SL–EA electrolytes rather than cathodic stability.

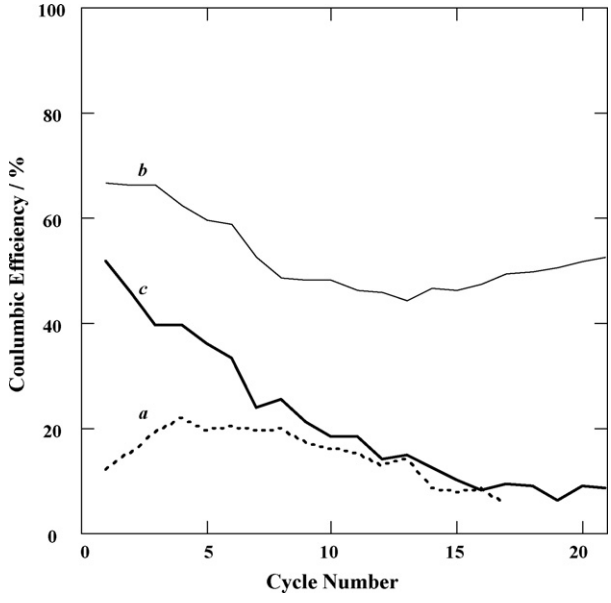

Fig. 10. Coulombic efficiency of Li/Pt cell, supporting electrolyte: 1 M $LiBF_4$, current density: 11 mA cm^{-2}, a(—): SL–MIB (1:1), b(—): IPMS–EA (1:1), c(—): SL–EA (1:1).

3.2.2.2. Addition of cycloalkane or triethylene glycol derivatives into SL–EA electrolytes. Addition of low reactivity surfactants of cycloalkanes or triethylene glycol derivatives into SL–EA electrolytes were investigated to lower the resistance of Li surface film. Decalin and adamantane were tested as cycloalkanes. Triethylene glycol dimethyl ether (triglyme), 1,8-bis(*tert*-butyldimethylsilyloxy)-3,6-dioxaoctane (TBDMSO) and triethylene glycol di(methanesulfonate) (TriglyMs) were tested. Chemical structure of these additives is shown in Fig. 11.

Cycloalkanes such as decalin or adamantane depress the formation of Li dendrite [25], and expected to act as surfactants on Li anode [26]. In our previous study, addition of adamantane was effective for improvement of Coulombic efficiency of Li/Pt cells with 1 M $LiClO_4$/PC [16].

Triglyme is also reported to be an effective additive to improve Coulombic efficiency of Li anode in $LiPF_6$–EC/EMC by adsorption of triglyme on Li surface [20]. In this work, three derivatives of triethylene glycols with different terminal groups were tested. Their Li^+ solvation properties are also expected

Table 3
Overpotential of Li/Pt cell with sulfone–ester electrolytes (supporting electrolyte: $LiBF_4$, current density: 11 mA cm^{-2}, electrode area: 0.09 cm^2)

Solvent	Additive	Overpotential (charge) (V[a])	Overpotential (discharge) (V[b])
SL–EA (1:1)	None	−0.44	0.22
IPMS–EA (1:1)	None	−0.13	0.12
SL–MIB (1:1)	None	−0.49	0.31
SL–EA (1:1)	Decalin (2 wt%)	−0.24	0.21
SL–EA (1:1)	Adamantane (saturated)	−0.31	0.29
SL–EA (1:1)	Triglyme (0.1 M)	−0.23	0.19
SL–EA (1:1)	TBDMSO (0.1 M)	−0.30	0.27
SL–EA (1:1)	TriglyMs (0.1 M)	−0.27	0.24
SL–EA (1:1)	VC (2 vol.%)	−0.24	0.21
EC–EMC (3:7)	None	−0.18	−0.15

[a] Voltage of the termination of charge (second cycle).
[b] Voltage of the initiation of discharge (second cycle).

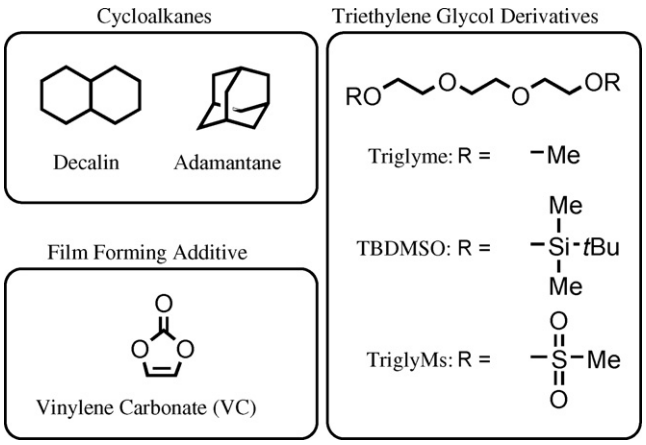

Fig. 11. Chemical structure of additives to attempt improvement of Coulombic efficiency of Li/Pt cell with SL–EA (1:1) electrolyte.

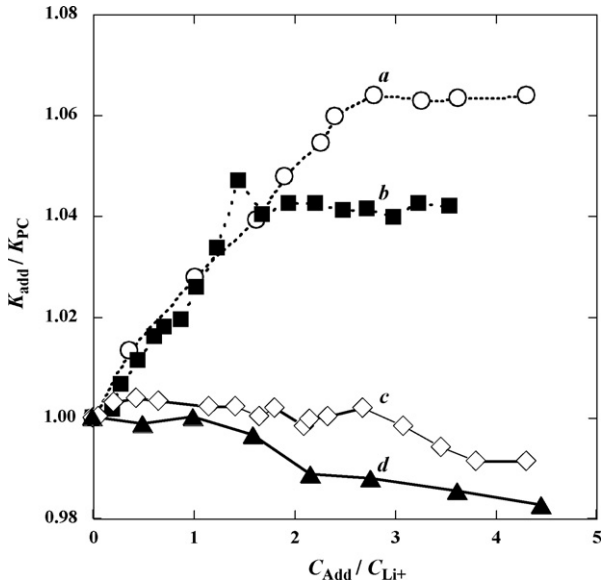

Fig. 12. Conductivity titration with polyether derivatives added 0.01 M $LiClO_4$/PC, a(○): triglyme, b(■): tetraethylene glycol dimethyl ether, c(□): TBDMSO, d(▲): TriglyMs, κ_{PC} = 213 μS cm^{-1} at 25 °C.

to differ. To evaluate the behavior of complex formation of triethylene glycol derivatives with Li^+, conductivity titration was performed (Fig. 12). These samples were dropped in 0.01 M $LiClO_4$/PC electrolyte. Then the ratio of conductivity values with and without additive (κ_{Add}/κ_{PC}) was plotted against the ratio of concentration of additive and Li^+ (C_{Add}/C_{Li^+}). Titration curve of triglyme shows saturation at the region of C_{Add}/C_{Li^+} is 2–3. This result indicates that two or three molecules of triglyme forms complex with one Li^+. On the other hand, TBDMSO and TriglyMs do not demonstrate formation of complex with Li^+ by this method.

Li cycling test results with addition of cycloalkanes or triethylene glycol derivatives are shown in Fig. 13. Addition of these compounds is effective for the improvement of Coulombic efficiency and depressing overpotential (Table 3). For cycloalkanes, average Coulombic efficiency for 1–20 cycles with SL–EA + adamantane or decalin was *ca.* 20% higher than that with SL–EA without additives (Fig. 13(A)). Effect of addition of cycloalkanes into SL–EA electrolytes system is clearer than that into $LiClO_4$/PC electrolyte [16]. From Fig. 13(B), average of Coulombic efficiency at 10–20 cycles with triethylene glycol derivatives increased *ca.* +10% regardless of the structure of terminal groups of triethylene glycol derivatives.

3.2.2.3. Addition of VC into SL–EA electrolytes. Vinylene carbonate (VC; Fig. 11) is an electrolyte additive, which can improve lithium cycling efficiency [27]. VC is easily reduced on surface of Li anode and surface film is formed. Li^+ ions can pass through this film and this film prevents the reduction of electrolyte. Then, addition of, reactive additive, VC into SL–EA electrolytes was examined in this work. Fig. 14(A) and (B) shows the Coulombic efficiency of Li/Pt cell and discharge capacity of Li/$LiCoO_2$ cell, respectively. For Li/Pt cell, Coulombic efficiency improved remarkably by addition of VC. It is equal to the Coulombic efficiency with EC–EMC (3:7). At the same time, overpotential is also decreased (Table 3). For Li/$LiCoO_2$ cell with SL–EA + VC, discharge capacity and Coulombic effi-

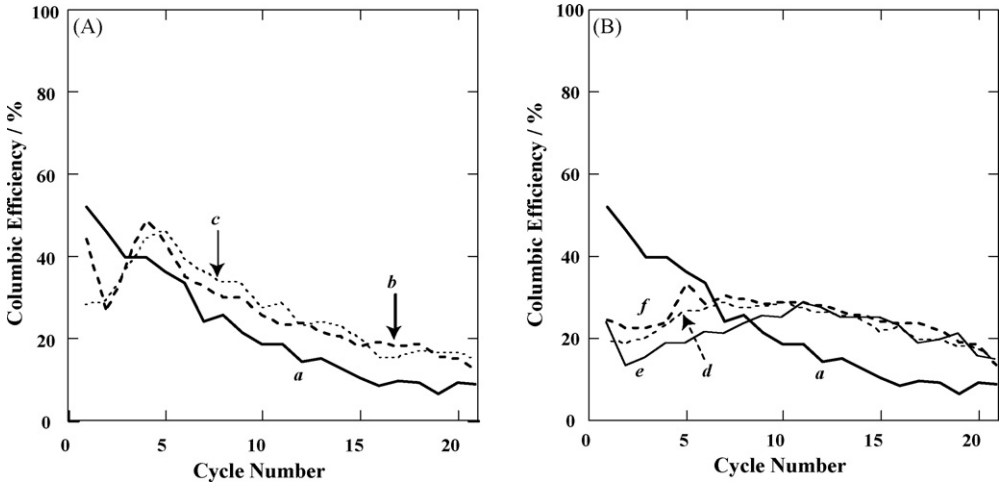

Fig. 13. Coulombic efficiency of Li/Pt cell with 1 M $LiBF_4$/SL–EA (1:1), (A) addition of cycloalkanes, (B) addition of triethylene glycol derivatives, a(—): no additive, b(—): 2 wt% decalin, c(—): saturated adamantane, d(—): 0.1 M triglyme, e(—): 0.1 M TBDMSO, f(—): 0.1 M TriglyMs.

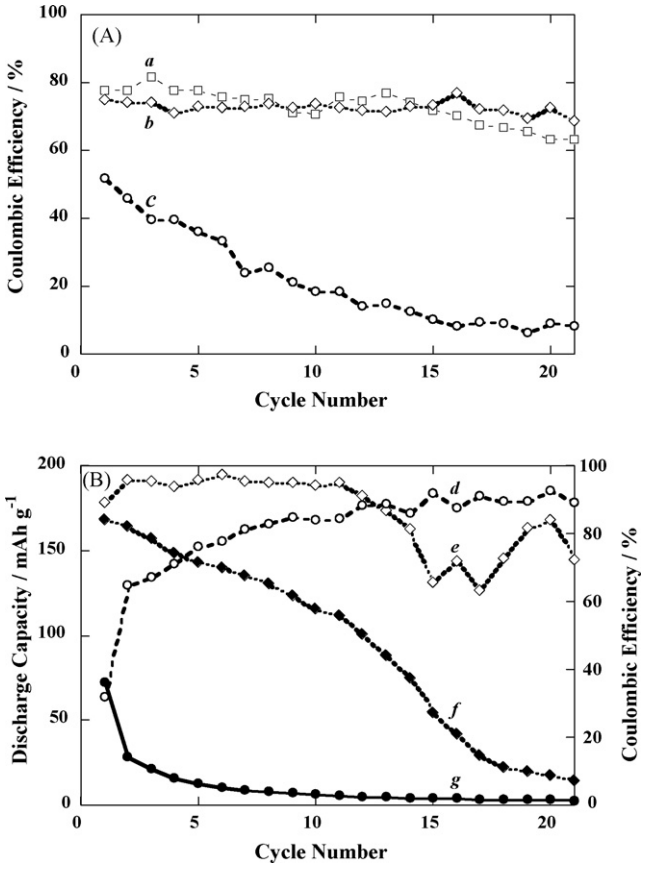

Fig. 14. (A) Coulombic efficiency of Li/Pt cell (supporting electrolyte: 1 M $LiBF_4$, current density: 11 mA cm^{-2}), a(□): EC–EMC (3:7), b(□): SL–EA (1:1) + 2 vol.% VC, c(◯): SL–EA (1:1) (no additive) and (B) Coulombic efficiency and discharge capacity of Li/$LiCoO_2$ cell (supporting electrolyte: $LiBF_4$, current density: 0.5 mA cm^{-2}, cut-off potential: 3–4.5 V), d(□): SL–EA (1:1) + 2 vol.% VC (Coulombic efficiency), e(◯): SL–EA (1:1) (no additive) (Coulombic efficiency), f(♦): SL–EA (1:1) + 2 vol.% VC (discharge capacity), g(●): SL–EA (1:1) (no additive) (Coulombic efficiency).

ciency also notably improved compared with SL–EA. However, discharge capacity and Coulombic efficiency of Li/$LiCoO_2$ cell with SL–EA + VC gradually decreased with an increase in cycle number. The difference of the effect of VC between Li/Pt cell and Li/$LiCoO_2$ cell is may be mainly due to the difference of the time to finish charge and discharge step. In our condition, Li/$LiCoO_2$ cell spends 2–3 h for charge step. On the other hand, Li/Pt cell needs only about 3 min to finish charge step. Therefore, Li/$LiCoO_2$ cell, chemical reaction between electrolyte and Li anode may proceed more than Li/Pt cells. Another possible reason may be some oxidation of electrolyte solution on cathode surface and/or cathode degradation at high charging cut-off voltage of 4.5 V. Due to the high cut-off voltage, discharge capacity of the cells exceed their theoretical capacity of $LiCoO_2$.

Fig. 15 shows Nyquist plot of charged Li/$LiCoO_2$ cells with and without VC. The first half-circle is regarded as the resistance of the interface of anode–electrolyte. For first to third cycle, the half-circle of Li/$LiCoO_2$ cells at low frequency side without VC risen up from *ca.* 50 to 100 Ω. In contrast, resistance of corresponding semi-circle of Li/$LiCoO_2$ cells with VC addition showed constant value of *ca.* 20 Ω contrast, even with an increase

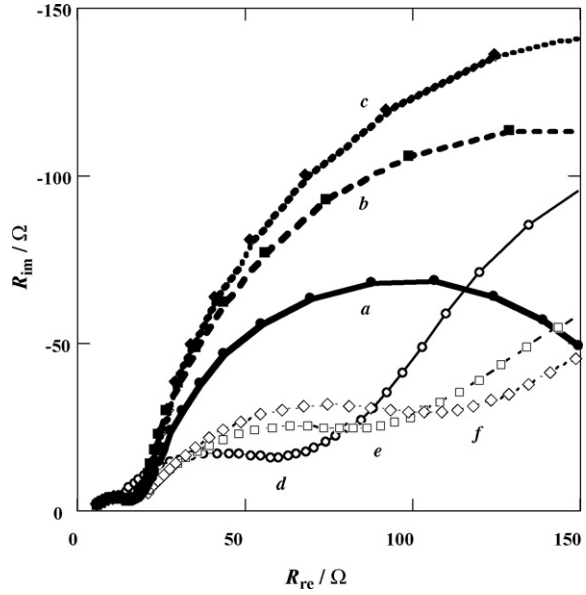

Fig. 15. Nyquist plots of charged Li/$LiCoO_2$ cell with $LiBF_4$/SL–EA (1:1), a(●): + 2 vol.% VC (first cycle), b(■): + 2 vol.% VC (second cycle), c(♦): +2 vol.% VC (third cycle), d(◯): no additive (first cycle), e(□): no additive (second cycle), f(□): no additive (third cycle).

in cycle number. These results suggest that the formation of VC film on Li anode occurred also in SL–EA electrolytes.

The effect of VC on improvement of cycling performance in SL–EA is also explained for another cell system, Li/$LiNi_{0.5}Mn_{1.5}O_4$ cell. Lithium cells with $LiNi_{0.5}Mn_{1.5}O_4$ cathode has been extensively studied as 5 V-class high-voltage cell. The cell with SL–EA + VC electrolyte was tested under the charge–discharge voltage region of 3–5 V (Fig. 16). Even on the condition of 5 V charge cut-off voltage, the cell with SL–EA + VC electrolyte kept the discharge capacity of *ca.* 130 mAh g^{-1} for 1–30 cycles. In contrast, discharge capacity of the cell without VC decreased rapidly in 1–10 cycles, and the Coulombic efficiency is unstable.

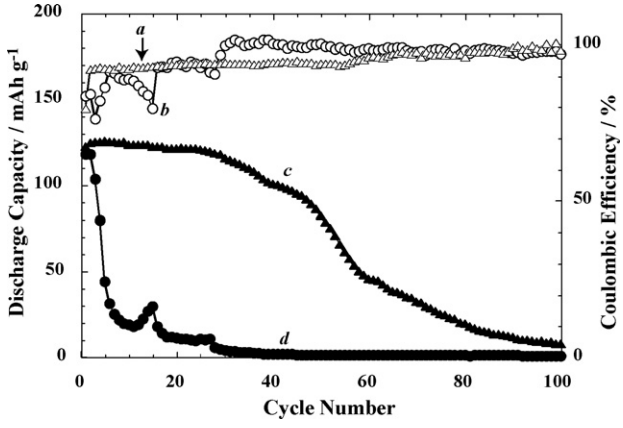

Fig. 16. Coulombic efficiency and discharge capacity of Li/$LiNi_{0.5}Mn_{1.5}O_4$ cell (supporting electrolyte: $LiBF_4$, current density: 0.5 mA cm^{-2}, cut-off potential: 3–5 V),), a(□): SL–EA (1:1) + 2 vol.% VC (Coulombic efficiency), b(◯): SL–EA (1:1) (no additive) (Coulombic efficiency), c(▲): SL–EA (1:1) + 2 vol.% VC (discharge capacity), d(●): SL–EA (1:1) (no additive) (Coulombic efficiency).

4. Conclusion

Sulfone–ester mixed solvent electrolytes were examined for 5 V-class high-voltage lithium cells. Through this study, electrolyte conductivity, electrochemical stability, solvation behavior of Li^+ ions and charge–discharge properties of $LiBF_4$/SL–EA electrolytes were investigated. Results of estimation of r_s by electrochemical methods and ^{13}C NMR measurements suggest that Li^+ ions are solvated both SL and EA. Anodic stability of SL–EA tends to be superior to EC–EMC electrolytes although the charge–discharge performance of the cell with lithium anode was poorer than that of EC–EMC electrolytes. Charge–discharge cycling property improved by using organic additives in electrolyte (*e.g.* cycloalkanes, triethylene glycol derivatives, and VC). Among these additives, VC addition was most effective not only for $Li/LiCoO_2$ cells with charge cut-off voltage of 4.5 V but also $Li/LiNi_{0.5}Mn_{1.5}O_4$ cells even with high charge cut-off voltage.

Sulfone–ester mixed solvent electrolyte system is expected to work as electrolyte system for 5–6 V-class high-voltage rechargeable lithium cells by further study on modification of using more adequate electrolyte additives or changing in chemical structure of solvents.

Acknowledgements

The authors wish to express their gratitude to Prof. Masafumi Unno and Dr. Shin-ichi Kondo of Gunma University for their helpful guidance and discussions regarding material preparation. The authors also thank Dr. Takeshi Yamanobe of Gunma University for helpful guidance and discussions about ^{13}C NMR spectra measurement.

References

[1] M. Takehara, R. Ebara, N. Nanbu, M. Ue, Y. Sasaki, Electrochemistry 71 (2003) 1172.
[2] M. Takehara, N. Tukimori, N. Nanbu, M. Ue, Y. Sasaki, Electrochemistry 71 (2003) 1201.
[3] M. Ue, K. Ida, S. Mori, J. Electrochem. Soc. 141 (1994) 2989.
[4] Q. Wang, S.M. Zakeeruddin, I. Exnar, M. Grätzel, J. Electrochem. Soc. 151 (2004) A1598.
[5] M. Watanabe, T. Kataoka, T. Fuchigami, H. Matsumoto, S. Hayase, S. Murai, T. Satou, H. Ohno, Ionsei Ekitaino Kinousouseito Ouyou, NTS, Tokyo, 2004, p. 67.
[6] K. Xu, C.A. Angell, J. Electrochem. Soc. 149 (2002) A920.
[7] X. Sun, C.A. Angell, Solid State Ionics 175 (2004) 257.
[8] X. Sun, C.A. Angell, Electrochem. Commun. 7 (2005) 261.
[9] T. Asahara, N. Tokura, M. Okawara, J. Kumanotani, M. Seno, Solvent Handbook, Kodansya Scientific, Tokyo, 1976, pp. 569, 625, 627, 768.
[10] J.J. Auborn, K.T. Ciemieki, Fall Meeting of ECS, 1983, p. 111 (Extended Abstract, 83-2).
[11] F. Ossola, G. Pistoia, S. Seeber, P. Ugo, Electrochim. Acta 33 (1988) 47.
[12] G. Viktor, The Donor–Acceptor Approach to Molecular Interactions, Gakkai Syuppan Center, Tokyo, 1983, pp. 22, 123.
[13] M. Yoshio, A. Akiya, Lithium-ion Batteries, 2nd ed., Nikkan Kogyo Shinbunsya, Tokyo, 2004, 84 pp.
[14] M.S. Newman, T.G. Barbee Jr., C.N. Blakesley, Z. Din, S. Gromelski Jr., V.K. Khanna, L. Lee, J. Radhakrishnan, R.L. Robey, V. Sankaran, S.K. Sankarappa, J.M. Springer, J. Org. Chem. 40 (1975) 2863.
[15] P.J. Kocienski, Protecting Groups, Corrected Edition, Georg Thieme Verlag, New York, 2000, 33 pp.
[16] Y. Watanabe, H. Morimoto, S. Tobishima, J. Power Sources 154 (2006) 246.
[17] Y. Watanabe, Y. Yamazaki, K. Yasuda, H. Morimoto, S. Tobishima, J. Power Sources 160 (2006) 1375.
[18] L.M. Mukherjee, D.P. Boden, R. Lindauer, J. Phys. Chem. 74 (1970) 1942.
[19] K.M. Abraham, D.M. Pasqudriello, F.J. Martin, J. Electrochem. Soc. 133 (1986) 661.
[20] S. Tobishima, H. Morimoto, M. Aoki, Y. Saito, T. Inose, T. Fukumoto, T. Kuryu, Electrochim. Acta 49 (2004) 979.
[21] R.A. Robinson, R.H. Stokes, Electrolyte Solutions, Butterworth Scientific Publications, London, 1995, 120 pp.
[22] K. Gering, T. Duong, in: K. Striebel (Ed.), Lithium/Lithium Ion Batteries, The Electrochemical Society Proceeding Series, Pennington, NJ, 2003.
[23] T. Fukushima, Y. Matsuda, H. Hashimoto, R. Arakawa, Electrochem. Solid State Lett. 4 (2001) A127.
[24] T. Fukushima, Y. Matsuda, H. Hashimoto, R. Arakawa, J. Power Sources 110 (2002) 34.
[25] J.O. Besenhard, J. Guurtler, P. Komenda, J. Power Sources 20 (1983) 253.
[26] L.A. Dominey, J.L. Goldman, V.R. Koch, Proc. Symp. Mater. and Processes for Lithium Batteries, 89-4, The Electrochem. Soc. Inc., 1989, pp. 213–222.
[27] H. Ota, K. Shima, M. Ue, J. Yamaki, Electrochim. Acta 49 (2004) 565.